Contribution of Intermolecular Interactions to Electron Transfer through Monolayers of Alkanethiols Containing Amide Groups

Slawomir Sek, Barbara Palys, and Renata Bilewicz*

Department of Chemistry, University of Warsaw, Pasteura 1, 02093 Warsaw, Poland

Received: October 19, 2001

Organothiol molecules with one or two amide moieties replacing the methylene groups in the alkyl chain were synthesized and self-assembled in mixed monolayers on the gold electrode. Structures of the monolayer films were studied by STM and electrochemical methods. Reflectance infrared spectroscopy confirmed the formation of intermolecular hydrogen bonds between the amide groups. In the case of diamides, the extent of hydrogen bonding in the external and internal planes of the monolayer were compared and both the odd and the even-membered molecules were considered. Impedance spectroscopy and chronoamperometry were employed to measure the electron transfer rate across mixed monolayers containing less than 10% of electroactive ferrocene organothiol with one or two amide groups in the chain. In the present paper, we focus on the amide location effects on kinetics of mediated electron transfer. Our results indicate that the distance between the planes where amide moieties are located and the electrode surface is of crucial importance. Deeply "buried" (i.e., located close to the electrode surface) amide groups were found to be responsible for the significant increase of electronic coupling comparing to simple *n*-alkanethiol monolayers. The effect of external amides was much less pronounced. This observation was explained as due to the different extent of hydrogen bonding in the internal and external plane of amide groups.

Introduction

Most experimental and theoretical studies of electron transport over distances aim to provide basis for the understanding of the relation between rate of electron transfer and the molecular structure of the medium separating the donor and acceptor. Usually, simple donor−acceptor models are employed, which neglect the important fact that the molecules occur in large and often well-organized molecular assemblies. In such supramolecular systems, not only the intramolecular interactions between the donor and acceptor of electrons in the molecule have to be considered, but also intermolecular van der Waals type interactions with the neighbor molecules may contribute to the electron-transfer efficiency.

This study explores monolayer systems where lateral intermolecular hydrogen bonding is responsible both for the efficiency of electron transfer and for the high stability of the monolayer coating the electrode substrate. Such ordered systems are of special utility for model studies of tunneling mechanisms in biological systems and microelectronic devices, and for further development of sensor technologies.

The structure dependent attenuation factor β expressing the decay of electronic coupling with the increase of distance separating the donor and acceptor should reflect also the nature of interactions with the immediate environment of the molecule under study. A wide range of β values are reported in the literature with the highest observed for photosynthetic reaction center − 1.4,[1] lower for saturated hydrocarbons and alkanethiols: 0.8−1.0,[2−8] and lowest for conjugated bridges, oligophenyleneethynylenes, or oligophenylenevinylenes (0.4−0.5).[9−11] The overall exponential decay constant $0.44-0.5A^{-1}$ reported for some proteins[12] and $0.60-0.65\ A^{-1}$ for organic glasses[13] indicates that through-bond coupling conceivable through covalent sigma-bonded bridges connecting the donor and acceptor cannot be the sole pathway for electron transport.

Recently, much attention has been paid to the influence of monolayer composition on the electron-transfer rate through the film. Replacement of one methylene link in the alkanethiol chain by ether, alkyne, or alkene groups resulted in reduction of the electron-transfer rate.[14] Introduction of ether link into both the electroactive component and the nonelectroactive diluent in the mixed monolayer lead also to a smaller but measurable decrease in the rate constant compared to that in the corresponding alkanethiol.[15] The reduction in the rate of electron transfer was ascribed to the reduced electronic coupling through the chain, and the influence of the ether links in the diluent suggested some contribution of electronic coupling through nonbonded contacts.

The main focus of research in our group is on the factors, which affect the order in the monolayers and the efficiency of electron transport through these layers. Recently, we have been involved in the studies of electron transport through the self-assembled monolayers with amide moieties replacing methylene units in alkyl chain, which appear to be more relevant to the biological electron transport systems than simple alkanethiols.[16] Sumner and co-workers have shown that single amide bond introduced into the electroactive molecule of a two-component monolayer with a simple alkanethiol as the nonelectroactive component does not increase the electronic coupling between the electrode and the redox center.[17] It is in agreement with our observation that the presence of amide bond affects electron tunneling through the monolayer only under conditions when

* To whom correspondence should be addressed. Fax: +48 22 8225996. E-mail: bilewicz@chem.uw.edu.pl.

10.1021/jp013896i CCC: $22.00
Published on Web 05/17/2002

it is able to form hydrogen bonds with the neighboring molecules.[16] The important feature of amide bonds is the possibility to form hydrogen bond network inside the SAM.[16−21] The presence of such internal hydrogen bond network could explain the increase of electron-transfer noted for amide containing SAMs.[16,22] In the present work, we describe long-range electron transfer to covalently attached redox-active centers (i.e., ferrocene) across two types of alkanethiolate monolayers containing one or two amide groups in place of selected methylene groups in the main alkyl chain. We try to understand the role of position of the amide moiety in the chain and of its lateral interactions for the properties of the monolayer and especially for the electronic coupling between the electroactive terminal group and the electrode.

Experimental Section

All compounds used in this work for syntheses were purchased from Aldrich and Fluka. Compounds **1**−**6** were synthesized according to earlier described procedures.[16] Confirmation of desired structures was provided by NMR and Mass spectra: **Compound 1.** $(S(CH_2)_2NHCO(CH_2)_{10}CH_3)_2$ − ^{1}H NMR ($CDCl_3$), δ (ppm): 0.88 (t, J = 7 Hz, 6H); 1.20−1.40 (broad overlapping resonance, 32H); 1.61 (m, 4H); 2.21 (t, J = 7 Hz, 4H); 2.83 (t, J = 6.5 Hz, 4H); 3.55 (m, 4H); 6.60 (broad s, 2H). Mass spectra (ESI-MS): m/z = 539.5 $[M+Na]^{\oplus}$. **Compound 2.** $(S(CH_2)_2NHCO(CH_2)_{13}CH_3)_2$ − ^{1}H NMR ($CDCl_3$), δ (ppm): 0.88 (t, J = 7 Hz, 6H); 1.25 (broad overlapping resonance, 44H); 2.21 (t, J = 6.5 Hz, 4H); 2.83 (t, J = 6.5 Hz, 4H); 3.57 (q, J = 6.5 Hz, 4H); 6.28 (broad s, 2H). Mass spectra (ESI-MS): m/z = 623.5 $[M+Na]^{\oplus}$. **Compound 3.** $(S(CH_2)_2NHCO(CH_2)_{10}NHCOCH_3)_2$ − ^{1}H NMR (CD_3OD), δ (ppm): 1.40−1.80 (broad overlapping resonance, 32H); 2.13 (s, 6H); 2.40 (t, J = 7 Hz, 4H); 3.05 (t, J = 7 Hz, 4H); 3.35 (m, 4H); 3.69 (m, 4H); 7.51 (weak); 7.91(weak). Mass spectra (ESI-MS): m/z = 625.5 $[M+Na]^{\oplus}$. **Compound 4.** $(S(CH_2)_2NHCO(CH_2)_{11}NHCOCH_3)_2$ − ^{1}H NMR (DMSO-d_6), δ (ppm): 1.20−1.60 (broad overlapping resonance, 36H); 1.77 (s, 6H); 2.05 (t, J = 7 Hz, 4H); 2.77 (t, J = 7 Hz, 4H); 2.99 (m, 4H); 3.31 (m, 4H); 7.64 (broad s, 2H); 7.86 (broad s, 2H). Mass spectra (ESI-MS): m/z = 653.4 $[M+Na]^{\oplus}$. **Compound 5.** $(S(CH_2)_2NHCO(CH_2)_{10}NHCOFc)_2$ − ^{1}H NMR ($CDCl_3$), δ (ppm): 1.20−1.70 (broad overlapping resonance, 32H); 2.22 (t, J = 7 Hz, 4H); 2.88 (t, J = 7 Hz, 4H); 3.56 (broad, 8H); 4.24 (s, 10H); 4.38 (s, 4H); 4.74 (s, 4H); 6.01 (broad s, 2H); 6.76 (broad s, 2H). Mass spectra (ESI-MS): m/z = 965.3 $[M+Na]^{\oplus}$. **Compound 6.** $(S(CH_2)_2NHCO(CH_2)_{11}NHCOFc)_2$ − ^{1}H NMR ($CDCl_3$), δ (ppm): 1.20−1.60 (broad overlapping resonance, 36H); 2.24 (t, J = 7 Hz, 4H); 2.88 (t, J = 7 Hz, 4H); 3.60 (broad, 8H); 4.24 (s, 10H); 4.36 (s, 4H); 4.69 (s, 4H); 6.03 (broad s, 2H); 6.72 (broad s, 2H). Mass spectra (ESI-MS): m/z = 993.4 $[M+Na]^{\oplus}$.

Monolayers were prepared on Au(111) substrates (Arrandee) which were used as working electrodes. The substrates were 200−300 nm thick gold films evaporated onto borosilicate glass precoated with 1−4 nm adhesion layer of Cr. Before adsorption of the monolayer, substrates were etched in hot nitric acid (for 10 min.) and then flame annealed in Bunsen burner. After this procedure, the electrodes were transferred to the coating solution. Self-assembly was carried out in ethanol solutions containing 0.1mM of electroactive disulfide (**5** or **6**) and 0.9 mM of proper diluent disulfide (**1**,**2**,**3**, or **4**). After 72 h of being soaked, the substrates were rinsed with ethanol and water.

Electrochemical experiments were performed in three-electrode system with Ag wire as a reference electrode and platinum foil as a counter electrode. The supporting electrolyte was 1M $HClO_4$. Water was distilled and passed through Milli-Q purification system. Cyclic voltammetry and chronoamperometry experiments were carried out using a Princeton Applied Research model 273A potentiostat, and impedance measurements were performed using Autolab PGSTAT30. All electrochemical measurements were carried out at 22 °C.

Infrared spectroscopy was performed with FTIR 8400 Shimadzu equipped with specular reflectance accessory—SpectraTech at 82° angle of incidence. Spectra were collected as 1000 averaged scans.

STM experiments were performed using Nanoscope IIIa (Digital Instruments, Santa Barbara, CA) and commercially available Pt−Ir tips. The images were taken under ambient conditions.

The monolayer assemblies studied by FTIR and STM were formed by nonelectroactive molecules.

Results

Structure of Monolayers. *Reflectance Infrared Spectroscopy.* The schemes of the monolayers studied in this work are presented in Figure 1. All systems contained amide moieties inserted into the alkyl chains of molecules forming the monolayer. SAM 1 and SAM 3 possess one plane of amide groups (internal) which are able to form hydrogen-bonded network within the monolayer.[18,19] SAM 2 and SAM 4 are formed by diamides; therefore, we can distinguish two planes of amide moieties—internal (located close to the electrode surface similar to SAMs 1 and 3) and external (located in the outer part of the monolayer). The ability to form hydrogen bonds in the plane of amides is connected with the odd−even position of amides, as shown by Schneider and co-workers.[21] In the present paper, these effects were investigated in the case of SAM 2 and SAM 4 using reflectance infrared spectroscopy. The spectra recorded for SAMs 2 and 4 are shown in Figure 2. The surface IR has been repeated for several identically prepared samples in order to verify the reproducibility. The characteristic band shapes, positions, and relative intensities for SAM 2 and SAM 4 are preserved. Consequently, we assume that both the layer deposition and the measurement of the IR spectra are reproducible. The valuable information about the structure of the monolayer can be extracted from the position of amide II band.[18,19] This band, in non-hydrogen-bonded state appears at ∼1510 cm^{-1}, whereas hydrogen bonding is reflected in a shift of the band to the higher wavenumbers ∼1530−1560 cm^{-1}. Analyzing spectra recorded for SAMs 2 and 4, we can observe two bands in amide II region. One of them appears at about 1511 cm^{-1} and second at about 1550 cm^{-1}. Such band split may result from the crystal field effect, however IR spectra of solid compounds 2 and 4 revealed the single amide II band at ∼1525 cm^{-1}. Therefore, in our opinion, the double amide II band indicates rather the existence of two different populations of amide groups within the monolayer, in hydrogen bonded and non-hydrogen bonded states. It is noteworthy that the ratio of these two bands is similar for SAM 2 and SAM 4 indicating that the fraction of hydrogen bonded amides in SAM 4 (ca. 59%), is not very different from that observed for SAM 2 (ca. 43%). If we compare this result with the spectra in the work of Schneider et al.,[21] we can conclude that the upper tier of amide moieties both in SAM 2 and in SAM 4 are not able to span the whole monolayer with a hydrogen-bonded network. The coexistence of hydrogen bonded together with nonbonded amide moieties is clearly

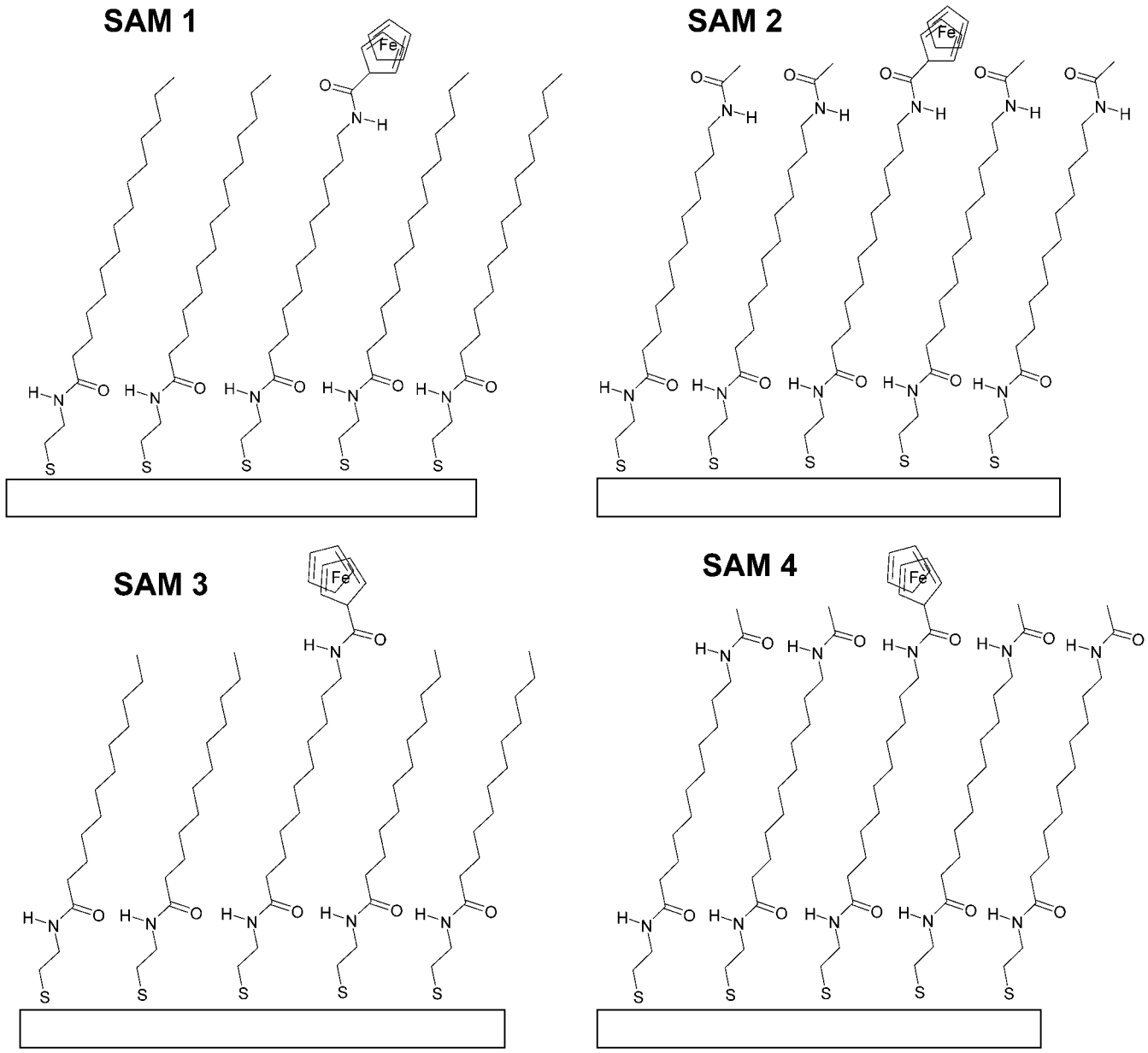

Figure 1. Scheme of the monolayer assemblies SAM 1−4.

visible for SAM 2. In the case of SAM 4, we observe a peak of the non-hydrogen-bonded state, despite suitable location of both amide planes because the external amides are in the even position relative to the internal amides. This has to be ascribed to the larger disorder in the outer plane of the monolayer assembly, compared to that close to the place where the monolayer is anchored to the electrode surface.

Figure 2 shows also FTIR spectra in C−H and N−H stretching region. The bands related with CH_3 group are very weak in comparison to alkanethiol spectra of comparable length.[19,23] Furthermore, the intensity ratio of CH_2 (sym) to CH_2 (asym.) is significantly decreased, what indicates more perpendicular orientation of molecules in diamide monolayers compared to simple *n*-alkanethiol systems.[24] Moreover, similarly to Schneider et al.[21] we did not observe amide A and B bands (in KBr at 3340 cm^{-1} and 3090 cm^{-1} respectively), as well as amide I band in spectra of SAM 4 (compound with even number of carbon atoms between amides). The absence of these bands may reflect the nearly parallel orientation of N−H and C═O bonds with respect to the gold surface. On the other hand, in the spectra of SAM 2 the very weak amide A band appearing at 3340 cm^{-1} may also reflect some nonuniformity in the orientation of amide groups in the monolayer.

Scanning Tunneling Microscopy. The structures of SAM 2 and SAM 4 were studied using STM technique. Figure 3 shows the STM images for bare gold and SAM 2 coated gold. Typical features such as single atom height steps and Au vacancy islands (dark spots in the image of Figure 3B) appear in these images. Figure 4 allows comparing molecularly resolved images of SAM 2 and SAM 4. The molecules form more linear structures than *n*-alkanethiols,[25−27] which can be connected with the arrangement of hydrogen bonds within the monolayer. The distance between the neighboring molecules in SAM 2 measured by STM is 5.5 ± 1.0 Å, slightly larger but still very close to the value reported for alkanethiolate monolayers (especially, if we consider the uncertainty in the determination of absolute distances measured by STM).[25−27] This observation indicates that the packing density of diamide molecules is similar to simple *n*-alkanethiol systems. It is in agreement with the results reported by Slowinski et al.[22] who found that the area per molecule in a monolayer of *n*-alkane-3-propanamides on Hg is about 20 $Å^2$, identical to that reported for *n*-alkanethiols.[6] The

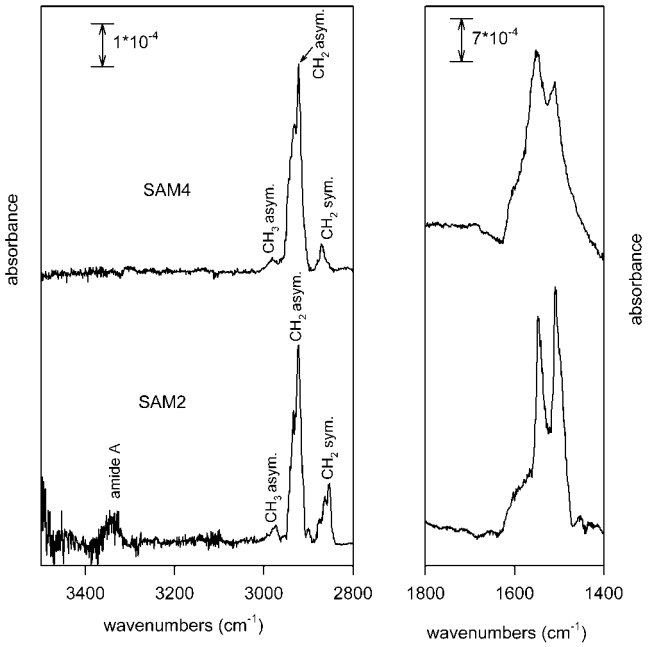

Figure 2. Reflectance infrared spectra recorded for SAM 2 (bottom) and SAM 4 (top). Two regions are shown: C−H(str) − left, and amide II − right.

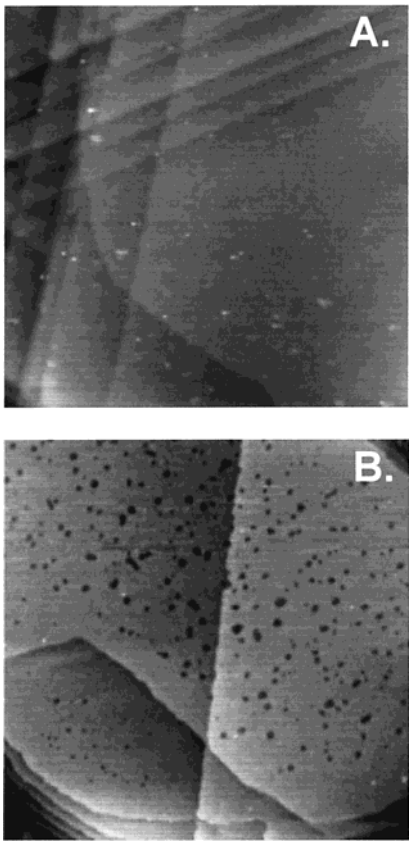

Figure 3. 3500 × 3500 Å STM images obtained for bare gold (A), and SAM 2 coated gold (B). Imaging conditions: $V_{sample} = +1V$; $I_t =$ 30 pA.

value found for diamide monolayer on gold is ca. 24 Å^2. The STM images for SAM 4 were similar to those obtained for SAM 2. In this case, we also observed the striped structure and the distances between neighboring molecules were ca. 5.5 Å. The direct comparison of STM images for SAM 2 (Figure 4A) and SAM 4 (Figure 4B) did not show any influence of odd−even

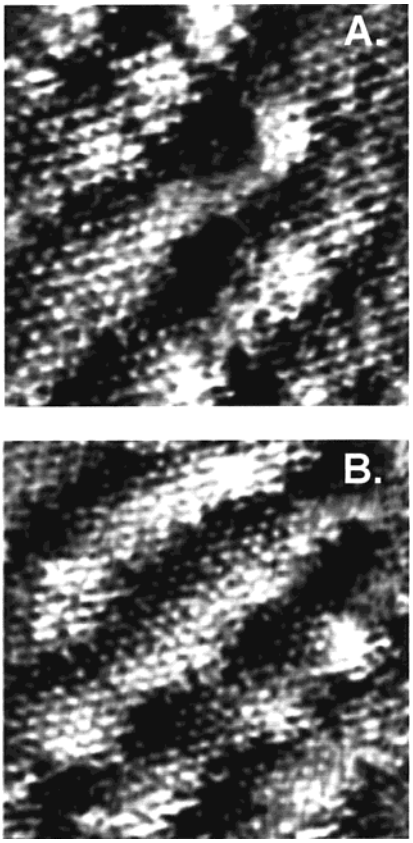

Figure 4. (A) 145 × 145 Å STM image of SAM 2. (B) 150 × 150 Å STM image of SAM 4. Imaging conditions: $V_{sample} = +1$V; $I_t = 1$ pA.

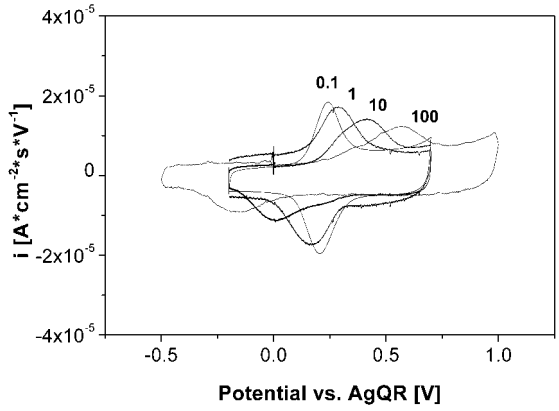

Figure 5. Cyclic voltammograms recorded in 1M $HClO_4$ for SAM 2 coated gold electrode. Scan rates: 0.1; 1; 10; 100 V/s.

position of the terminal amide in the chain on the structure of the diamide monolayers.

Electrochemical Studies. SAMs 1−4 were studied using cyclic voltammetry. Figure 5 shows typical current−potential curves for SAM 2 recorded at 0.1; 1; 10; 100 V/s. On the basis of voltammograms recorded at low scan rates (0.02−0.1 V/s), formal potentials for each system were determined. The results are shown in Table 1. Formal potentials for SAM 1 and SAM 3 are slightly more positive compared to values obtained for SAM 2 and SAM 4. This effect can be explained if we consider the environment surrounding the ferrocene redox centers in monolayers. In SAM 1 and SAM 3, ferrocene moieties are located in close neighborhood of nonpolar alkyl groups, while in SAM 2 and SAM 4 these groups are replaced with $NHCOCH_3$, which are more polar than the alkyl groups. The different environment around the redox center explains the

TABLE 1: Formal Potentials for SAMs Obtained from Cyclic Voltammetry Experiments

monolayer	formal potential [V] vs SSCE
SAM 1	$+0.37 \pm 0.01$
SAM 2	$+0.32 \pm 0.01$
SAM 3	$+0.36 \pm 0.02$
SAM 4	$+0.33 \pm 0.02$

differences in the formal potentials with a shift of formal potentials to more positive values for the more hydrophobic surrounding of ferrocene in case of SAM 1 and 3 (Table 1).[28] On the basis of voltammetric experiments (from the area of oxidation peak) we determined the percentage of electroactive molecules in the monolayer assembly. For SAMs studied in this work, it was always lower than 10%. Higher contents of electroactive component in the monolayer could not be used because they lead to the repulsion of ferrocene moieties evidenced by an increase of half-height width of the voltammetric peaks and phase separation of monolayer components observed also in mixed monolayers of these two components in the Langmuir monolayers on the water−air interface.[29]

The values of double-layer capacitances for SAMs 1−4 were obtained using the impedance technique.[30−33] Capacitances were measured at −0.1 V vs AgQR, in a region where the faradaic processes did not occur. A typical complex plane impedance plot and Bode plot obtained from these experiments are shown in Figure 6. All SAMs reported in this study showed the behavior of capacitors at double layer region, exhibiting the phase angles equal or higher than 87° (Figure 6B). The equivalent circuit employed for the determination of double-layer capacitance consists of a resistor and constant phase element in a series. The values obtained from these experiments are shown in Table 2. The double layer capacitances for bare gold and hexadecanethiol coated electrodes are also included in the table. The values of capacitance obtained for amide containing monolayers are larger than for the corresponding *n*-alkanethiolate systems with analogous thickness. It is not an indication that amide containing SAMs are less ordered, but is rather due to the different dielectric properties − the dipole moment of the amide moiety leads to a change of the dielectric constant of the monolayer. Significant difference in the dipole moments was found for Langmuir monolayers of Au clusters modified with $S(CH_2)_2NHCO(CH_2)_{13}CH_3$, and respective alkanethiol.[29] A large change in the effective dielectric constant of the film was reported for ether-linked chains compared to the alkanethiol layers.[15] It is also interesting to compare the values of double-layer capacitance for amide SAMs with other systems formed by molecules with polar groups. For example, the values of double layer capacitance, for monolayers with COOH or $COOCH_3$ terminal groups,[34] are similar to those obtained by us for diamide SAMs. Based on the above results, the monolayers studied exhibit high degree of order, which makes them suitable for further studies of long-range electron transfer across the monolayer.

Kinetics of Electron Transfer through Monolayers Containing Amide Groups. Recently, we have shown that the introduction of amide moieties into the alkane chains of the molecules leads to the increase of electron-transfer efficiency across this monolayer.[16a] However, this effect is obtained only under conditions when the amide moieties are able to generate hydrogen bonds between the neighboring molecules, hence mixed monolayers have to be employed with the diluent thiol also possessing the amide group in the same place of the chain. In another paper, we demonstrated that introduction of a second

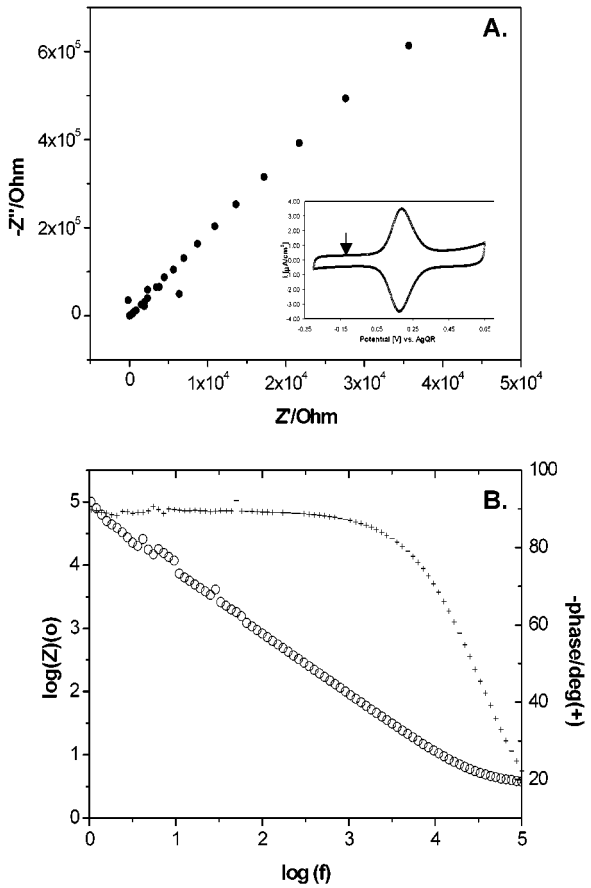

Figure 6. A. Complex plane impedance plot recorded at −0.1V vs AgQR, for SAM 4 modified gold electrode. Inset shows cyclic voltammogram for SAM 4, the arrow indicates the potential where the double-layer capacitance was measured. B. Bode plot for SAM 2, frequency range: 1 Hz−100 kHz, $E = -0.1$V vs AgQR, amplitude: 0.01 V.

TABLE 2: Double-Layer Capacitance for SAMs Modified Gold Electrodes

electrode	capacitance [μF/cm^2]
bare Au (111)	19.6 ± 0.9
SAM of C16SH	1.09 ± 0.21
SAM1	2.39 ± 0.30
SAM2	2.86 ± 0.37
SAM3	6.25 ± 0.37[a]
SAM4	2.91 ± 0.33

[a] The capacitance is repeatedly higher than for other SAMs.

amide plane in the outer part of a nonelectroactive monolayer does not affect significantly the rate of electron transfer across the layer.[16b] This observation was explained as due to the inappropriate ("odd") position of amide moieties in the outer plane of the monolayer, which resulted in difficulty in the formation of intermolecular hydrogen bonds. However, this hypothesis could not be verified experimentally because only molecules with odd positioned amides were available at that time. In the present paper, we pay attention to the effect of the position of the amides in the outer plane on the electron transfer efficiency and therefore, four different types of monolayers were compared in pairs: SAM 1 with SAM 2 and SAM 3 with SAM 4 (Figure 1). The monolayers compared in one pair contain the same electroactive molecule with a ferrocene terminal group and differ only by the number of amides in the chains of the electroinactive diluent molecules. For SAM1 and SAM 3, only one − internal amide plane is formed, whereas for SAM 2 and 4, two amide planes are present in the monolayer.

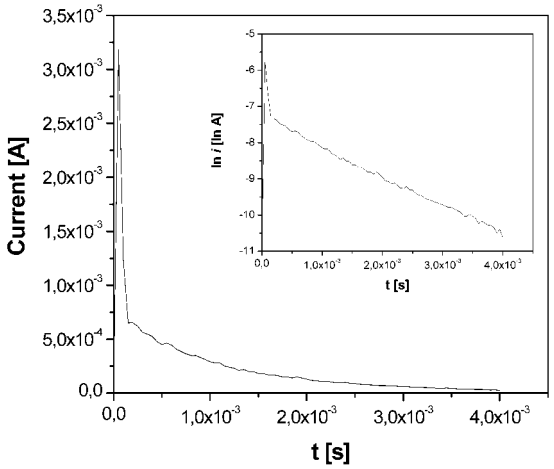

Figure 7. Chronoamperometric curve recorded in 1M $HClO_4$ for SAM 3 at overpotential −0.15 V. Inset shows dependence of ln *i* vs *t*.

The kinetic parameters (rate constants and reorganization energies) for the electron transfer through the systems studied were determined using electrochemical methods: chronoamperometry and impedance spectroscopy. In the former case, the rest potential and the potential at which the current was recorded were symmetric relative to the formal potential of the immobilized ferrocene group. The apparent ET rate constant is calculated based on the equation[3]

$$i = k_{app} Q \exp(-k_{app} t) \tag{1}$$

The rate constant is obtained from the slope of ln *i* vs *t* plot. Linearity of this plot confirms that all or at least majority of centers are located in the same distance from the electrode surface which in turn convinces about the uniformity and order in the layer (Figure 7). The values of rate constants determined at various overpotentials allowed to obtain the standard rate constant. Experimental dependencies of ln k_{app} vs η were fitted to the theoretical Tafel plots obtained on the basis of the Marcus theory[35,36]

$$k_{app} = \upsilon \rho k_B T \int_{-\infty}^{+\infty} \frac{\exp\left\{-\left(\frac{k_B T}{4\lambda}\right)\left[x - \frac{\lambda \pm e\eta}{k_B T}\right]^2\right\}}{1 + \exp(x)} dx \tag{2}$$

where υ is the distance dependent electronic coupling between the electrode and the redox sites; ρ is the density of electronic states in the metal of the electrode; λ is the reorganization energy; η is the overpotential; k_B is the Boltzmann constant; *x* is the electron energy relative to the Fermi level; *T* is the temperature and *e* is the charge of an electron. On the basis of the fitting procedure the rate constants at zero overpotential and reorganization energies were evaluated. Representative Tafel plot is shown in Figure 8.

In the impedance experiments the procedure of Brevnov and Finklea was employed.[37] Kinetic parameters were determined from fits of experimental admittance data to theoretical curves obtained on the basis of Laviron treatment (for covalently bonded, strongly adsorbed species in the limit of small ac potential perturbation and assuming the absence of intermolecular interactions).[38] The faradaic impedance is represented as a series combination of frequency-independent R_a and C_a, where R_a and C_a are adsorption resistance and capacitance respectively, which are given by eqs 3 and 4. Equations 5 and 6 describe the superficial surface concentrations of the Ox and Red forms in the absence of ac current. Equation 7 relates the

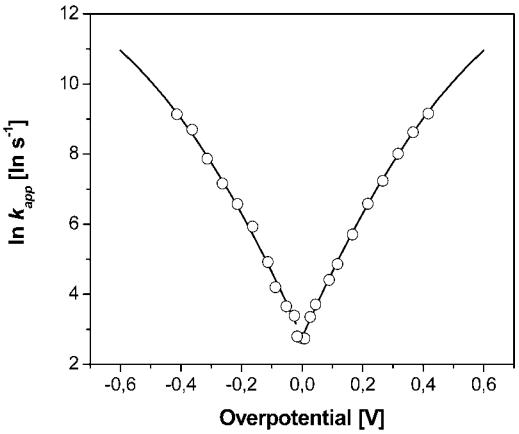

Figure 8. Tafel plot for SAM 2. Theoretical plot (line) was calculated using eq 2, points are experimental data.

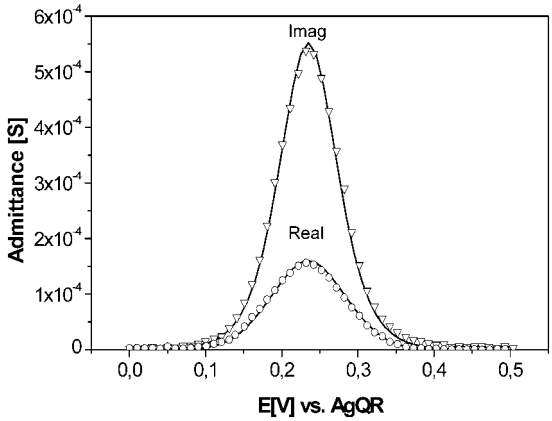

Figure 9. Faradaic admittance for SAM 2 at $f = 20$ Hz. Points are experimental data. Theoretical fits are shown as lines.

faradaic admittance with R_a and C_a

$$R_a = \left(\frac{RT}{n^2 F^2 A k_s}\right)[\alpha \Gamma_o \eta^{-\alpha} + (1-\alpha)\Gamma_r \eta^{1-\alpha}]^{-1} \tag{3}$$

$$(C_a)^{-1} = k_s R_a (\eta^{-\alpha} + \eta^{1-\alpha}) \tag{4}$$

$$\Gamma_o + \Gamma_r = \Gamma_{total} \tag{5}$$

$$\Gamma_o/\Gamma_r = \eta = \exp\left(\frac{nF(E_{dc} - E^{o\prime})}{RT}\right) \tag{6}$$

$$Y^{faradaic} = (Z^{faradaic})^{-1} = \left(R_a - \frac{j}{\omega C_a}\right)^{-1} \tag{7}$$

Representative results of the fitting of the experimental admittance vs potential to the theoretical plots are shown in Figure 9.

The results obtained by the two methods (CA and Impedance) are collected in Table 3. The values of reorganization energies are in the range 0.81−0.84 eV, which is in agreement with the literature data for monolayers containing ferrocenes.[35,39] Small deviations may reflect the differences in the dielectric constants in the monolayers and in the immediate surrounding of electroactive groups or may be result of small differences in the thickness of the layers. The interesting conclusion comes out of the comparison of rate constants SAM 1 and SAM 2 (Table 3). Similar values of rate constants mean that introduction of additional amide group plane does not bring any change in

TABLE 3: Kinetic Parameters Determined for SAMs 1−4

monolayer	reorganization energy [eV][a]	rate constant [s^{-1}][a]	rate constant [s^{-1}][b]
SAM 1	0.83 ± 0.02	18 ± 2	24 ± 4
SAM 2	0.84 ± 0.01	19 ± 2	21 ± 4
SAM 3	0.81 ± 0.01	57 ± 3	57 ± 3
SAM 4	0.84 ± 0.01	51 ± 3	68 ± 3

[a] Chronoamperometry experiments. [b] Impedance experiments.

the electron transport efficiency. This result agrees with the one presented in our recent paper for nonelectroactive systems.[16b] It was explained assuming that hydrogen bonding could not be formed in the outer layer of SAM2. If the outer amide groups were situated in the "even position" relative to the amide groups in the inner plane, based on molecular modeling, the formation of hydrogen bonds could be expected. However, experimentally, the enhancement of electron-transfer efficiency was not observed upon adding the second plane of amides. The comparison of kinetic parameters for SAM 3 and SAM 4 (Table 3) demonstrates that the efficiency of electron transfer is comparable, confirming that in the outer tier, the most of NHCO groups are not bonded by the hydrogen bonds. In our opinion, the large distance of the second amide plane from the electrode surface may be explaining lack of extensive hydrogen bonding even for SAM 4, as due to the higher degree of disorder in the outer plane compared to the internal plane of amides. However, this disorder may be considered as a result of the twist of adsorbed molecules, which prevents the hydrogen bonding in the upper tier of the amides.[24] This would explain the different behavior of amides in the internal and external part of the monolayer.

Discussion

The presence of amide bonds in the outer part of the monolayer did not affect the rate of electron transfer across the monolayer in contrary to the hydrogen-bonded amides buried inside the monolayer. Introduction of hydrogen bonded network into the monolayer causes more efficient electron-transfer comparing to simple methylene bridges. It should be noted that replacement of methylene link in the monolayer by ether moieties reported by Napper et al.[15] lead to an opposite result − reduction of rate of electron transfer compared to that in monolayers of simple alkanethiols. According to these authors, the nonnearest neighbor coupling between chains may be important for the overall electronic coupling through compact film. The nonnearest neighbor coupling between chains may be of similar magnitude as that between two orbitals on the same chain.[15] The authors explain the difficulty in proving this experimentally for the thiols with ether linkages as due to difficulty in disentangling the effects of interchain coupling from changes in the dielectric constant upon inserting the ether units into the chains. According to the authors the difficulty in detecting interchain contribution may also reflect the better defined geometry between the orbital sites in the same chain compared to those between chains. In contrary, in our systems, the presence of internal amide groups in the monolayer is shown to contribute to the electron-transfer efficiency. Increase of rate constant compared that for a corresponding thiol monolayer is always obtained. This is ascribed to the role of lateral hydrogen bonding close to the electrode surface where the ordering of the layer is better defined and the geometry of the sites in the neighboring chains may become appropriate for the overlapping of orbitals.

To demonstrate the enhanced efficiency of electron tunneling through hydrogen bonded amides we consider SAM 1 as three

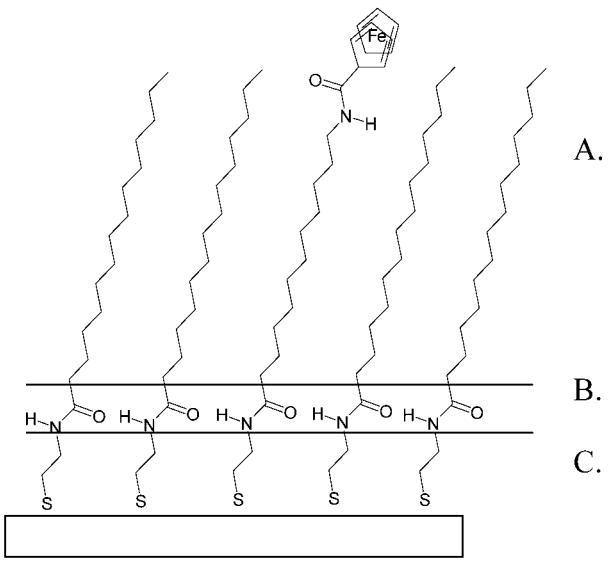

Figure 10. Scheme of the SAM 1 treated as three superimposed layers of different electron mediating properties.

superimposed layers of different electron mediating properties as shown in Figure 10. Similar model was applied by Holmlin and co-workers for metal−insulator-metal tunneling junction consisting of two alkanethiolate monolayers.[40] The rate constant, k along the whole chain can be described by equation

$$k = k^0 \exp(-\beta n) \tag{8}$$

where k^0 is the rate constant in the absence of the monolayer, β is the tunneling constant and n is the number of atoms separating the redox center from the electrode. If our monolayer is treated as a series of three different sublayers (Figure 10) the electron passes part A where β_A is $1.2/CH_2$ then part B where the decay constant is not known and next part C where $\beta_C = \beta_A = 1.2/CH_2$. The electron-transfer rate can be described by equation

$$k_{ABC} = k^0 \exp(-\beta_A n_A - \beta_B n_B - \beta_C n_C) \tag{9}$$

We assume here that the length of amide group equals to two methylene groups, therefore n_A, n_B, n_C corresponds to the number of atoms in layers A, B, and C, respectively. In eqs 8 and 9 ,the unknowns are k^0 and β_B. The first parameter should be identical to that determined for a simple alkanethiol system, hence, not containing internal hydrogen bonding. The electroactive group has to be the same and the diluent is simple thiol $C_{16}SH$. From our recent study[16a] the k value for such a system was found to be 4.5 s^{-1}. On the basis of this result, using eq 8, we are able to determine the value of k^0. The value of tunneling constant used to determine k^0 is $\beta = 1.2/CH_2$. The number of atoms n was taken as equal 15 − the sulfur atom and amide group involved in the ferrocene tether were omitted in this consideration because the length of the Au−S and N−C bonds corresponds approximately to the distance of the closest approach for ferrocene moiety in redox reaction between the electrode and untethered (soluted) ferrocene.[4] Using these data, we obtain the k^0 value 3×10^8 s^{-1} in agreement with the literature.[4] If this value is known, we are able to calculate the decay constant β_B. In SAM 1, similarly as in the simple alkanethiol system considered above, the whole chain consists of $n = 15$ atoms. In part A, the number of atoms is $n_A = 11$, in part B, n_B is 2 and in part C, n_C is also 2. The value of k_{ABC} was found here to be 18 s^{-1} so based on eq 9 we obtain $\beta_B =$

0.5 per unit. Thus, the efficiency of tunneling is increasing when internal hydrogen bonds strengthen lateral interactions within the monolayer. The decay value is twice smaller through the amide groups involved in the hydrogen network than along simple methylene units. The role of noncovalent bonded superexchange interactions between neighboring molecules located at small distances from the electrode seems to be of primary importance for the electronic coupling through well organized molecular films. It should be stressed that the model presented above is simplified. It assumes that the tunneling decay terms are simply multiplication of exponentials thus, order functionalities in the chain are neglected. On the other hand, we assume that the main mechanism of electron tunneling is through σ bonds and, therefore, different orientation of molecules forming the monolayer should not influence significantly the rate of electron transfer.[6] Our model aims to show that there is a difference of tunneling decay when amides are able to form lateral hydrogen bond network and the electron density on amide group is changed by the interchain hydrogen bond interactions.

Acknowledgment. This work was supported by KBN Grant No. 3T09A 12219.

References and Notes

(1) Moser, C. C.; Keske, J. M.; Warncke, K.; Farid, R. S.; Dutton, P. L. *Nature* **1992**, *335*, 796.
(2) Becka, A. M.; Miller, C. J. *J. Phys. Chem.* **1992**, *96*, 2657.
(3) Finklea, H. O.; Hanshew, D. D. *J. Am. Chem. Soc.* **1992**, *114*, 3173.
(4) Smalley, J. F.; Feldberg, S. W.; Chidsey, C. E. D.; Linford, M. R.; Newton, M. D.; Liu, Y.-P. *J. Phys. Chem.* **1995**, *99*, 13 141.
(5) Finklea, H. O.; Liu, L.; Ravenscroft, M. S.; Punturi, S. *J. Phys. Chem.* **1996**, *100*, 18 852.
(6) Slowinski, K.; Chamberlain, R. V.; Miller, C. J. K.; Majda M. *J. Am. Chem. Soc*. **1997**, *119*, 11 910.
(7) Weber, K.; Hockett, L.; Creager, S. E. *J. Phys. Chem. B* **1997**, *101*, 8286.
(8) Kasmi, A. E.; Wallace, J. M.; Bowden, E. F.; Binet, S. M.; Linderman, R. J. *J. Am. Chem. Soc*. **1998**, *120*, 225.
(9) Sachs, S. B.; Dudek, S. P.; Hsung, R. P.; Sita, L.; Smalley, J. F.; Newton, M. D.; Feldberg, S. W.; Chidsey, C. E. D. *J. Am. Chem. Soc*. **1997**, *119*, 10 563.
(10) Creager, S.; Yu, C. J.; Bamdad, C.; O'Connor, S.; MacLean, T.; Lam, E.; Chong, Y.; Olsen, G. T.; Luo, J.; Gozin, M.; Kayyem, J. F. *J. Am. Chem. Soc*. **1999**, *121*, 1059.
(11) Sikes, H. D.; Smalley, J. F.; Dudek, S. P.; Cook, A. R.; Newton, M. D.; Chidsey, C. E. D.; Feldberg S. W. *Science* **2001**, *291*, 1519.
(12) Kuki, A. *Structure and Bonding* **1991**, *75*, 49.
(13) Closs, G. L.; Miller, J. L. *Science* **1988**, *240*, 440.
(14) (a) Sinniah, K.; Cheng, J.; Terrettaz, S.; Reutt-Robey, J. E..; Miller, C. J. *J. Phys. Chem.* **1995**, *99*, 14 500. (b) Cheng, J.; Saghi-Szabo, G.; Tossel, J. A.; Miller, C. J. *J. Am. Chem. Soc.* **1996**, *118*, 680.
(15) Napper, M. A.; Liu, H.; Waldeck, D. H. *J. Phys. Chem. B* **2001**, 105, 7699.
(16) (a) Sek, S.; Misicka, A.; Bilewicz, R. *J. Phys. Chem. B* **2000**, 104, 5399. (b) Sek, S.; Bilewicz, R. *J. Electroanal. Chem.* **2001**, *509*, 11.
(17) Sumner J. J.; Weber, K. S.; Hockett, L. A.; Creager, S. E. *J. Phys. Chem. B* **2000**, *104*, 7449.
(18) Tam-Chang, S.-W.; Biebuyck, H. A.; Whitesides, G. M.; Jeon, N.; Nuzzo, R. G. *Langmuir* **1995**, *11*, 4371.
(19) (a) Clegg, R. S.; Hutchison, J. E. *Langmuir* **1996**, *12*, 5239. (b) Clegg, R. S.; Reed, S. M.; Hutchison, J. E. *J. Am. Chem. Soc*. **1998**, *120*, 2486. (c) Clegg, R. S.; Hutchison, J. E. *J. Am. Chem. Soc*. **1999**, *121*, 5319 (d) Clegg, R. S.; Reed, S. M.; Smith, R. K.; Barron, B. L.; Rear, J. A.; Hutchison, J. E. *Langmuir* **1999**, *15*, 8876, (e) Smith, R. K.; Reed, S. N.; Lewis P. A.; Monnell, J. D.; Clegg, R. S.; Kelly, K. F.; Bumm, L. A.; Hutchison, J. E.; Weiss, P. S. *J. Phys. Chem.* B **2001**, *105*, 1119.
(20) Sabapathy, R. C.; Bhattacharyya, S.; Leavy, M. C.; Cleland Jr., W. E.; Hussey, C. L. *Langmuir* **1998**, *14*, 124.
(21) Schneider, J.; Messerschmidt, C.; Schulz, A.; Gnade, M.; Schade, B.; Luger, P.; Bombicz, P.; Hubert, V.; Fuhrhop, J.-H. *Langmuir* **2000**, *16*, 8575.
(22) Slowinski, K.; Fong, H. K. Y.; Majda, M. *J. Am. Chem. Soc*. **1999**, *121*, 7257.
(23) Porter, M. D.; Bright, T. B.; Allara, D. L.; Chidsey, C. E. D. *J. Am. Chem. Soc*. **1987**, *109*, 3559.
(24) Comparison of the intensities of selected infrared bands of the monolayer referenced to those of bulk sample allows us to estimate the twist and tilt angle of the molecules forming the monolayer (see eqs 5−7 in ref 14a). The values obtained are 60° and 15° for twist and tilt angles, respectively. The values of twist and tilt angles were similar for SAM 2 and SAM 4. These results should be, however, treated only as approximation, because direct comparison of amide II bands for monolayer and bulk sample is difficult due to the fact that intensities of these bands are strongly affected by the extent of hydrogen bonding. The latter may be different within the monolayer and the bulk phase sample.
(25) Schonenberger, C.; Sondag-Huethorst, J. A. M.; Jorritsma, J.; Fokkink, L. G. J. *Langmuir* **1994**, *10*, 611.
(26) (a) Poirier, G. E.; Tarlov, M. J. *Langmuir* **1994**, *10*, 2853, (b) Poirier, G. E. *Chem. Rev.* **1997**, *97*, 1117.
(27) Sprik, M.; Delamarche, E.; Michel, B.; Rothlisberger, U.; Klein, M. L.; Wolf, H.; Ringsdorf, H. *Langmuir* **1994**, *10*, 4116.
(28) (a) Creager, S. E.; Rowe, G. K. *Anal. Chim. Acta* **1991**, *246*, 233. (b) Creager, S. E.; Rowe, G. K. *J. Electroanal. Chem.* **1998**, *420*, 291.
(29) (a) Bilewicz, R.; Sek, S.; Zawisza, I. *Russ. J. Electrochem*. **2002**, *38*, 29. (b) Bilewicz, R.; Sek, S.; Zawisza, I., to be submitted.
(30) Lasia, A. Electrochemical Impedance Spectroscopy and its Applications. In *Modern Aspects of Electrochemistry*; Conway, B. E., Bockris, J. O'M., White, R. E.; Eds.; Kluwer Academic/Plenum Publishers: New York, 1999; pp. 143−242.
(31) Janek, R. P.; Fawcett, W. R.; Ulman, A. *J. Phys. Chem. B* **1997**, *101*, 8550.
(32) Protsailo, L. V.; Fawcett, W. R. *Electrochim. Acta* **2000**, *45*, 3497.
(33) Boubour, E.; Lennox, R. B. *Langmuir* **2000**, *16*, 4222.
(34) Finklea, H. O. Electrochemistry of Organized Monolayers of Thiols and Related Molecules on Electrodes. In *Electroanalytical Chemistry*; Bard, A. J., Rubinstein, I.; Eds.; Marcel Dekker: New York, 1996; pp 109−335.
(35) (a) Marcus, R. A. *J. Phys. Chem.* **1963**, *67*, 853. (b) Marcus, R. A. *J. Chem. Phys*. **1965**, *43*, 679.
(36) Chidsey, C. E. D. *Science* **1991**, *251*, 919.
(37) Brevnov, D. A.; Finklea, H. O. *J. Electrochem. Soc.* **2000**, *147*, 3461.
(38) Laviron, E. *J. Electroanal. Chem.* **1979**, *97*, 135.
(39) (a) Weber, K.; Creager, S. E. *Anal. Chem*. **1994**, *66*, 3164. (b) Weber, K.; Creager, S. E. *J. Electroanal. Chem*. **1998**, *458*, 17.
(40) Holmlin, R. E.; Haag, R.; Chabinyc, M. L.; Ismagilov, R. F.; Cohen, A. E.; Terfort, A.; Rampi, M. A.; Whitesides, G. M. *J. Am. Chem. Soc*. **2001**, *123*, 5075.